Available online at www.sciencedirect.com
ScienceDirect
Trans. Nonferrous Met. Soc. China 22(2012) 111−116

Transactions of Nonferrous Metals Society of China
www.tnmsc.cn

Effect of $MoSi_2$ content on dielectric and mechanical properties of $MoSi_2/Al_2O_3$ composite coatings

WU Zhi-hong, ZHOU Wan-cheng, LUO Fa, ZHU Dong-mei

State Key Laboratory of Solidification Processing, Northwestern Polytechnical University, Xi'an 710072, China

Received 27 December 2010; accepted 19 September 2011

Abstract: Molybdenum disilicide ($MoSi_2$) sheath and aluminum oxide (Al_2O_3) core blended powders were fabricated by spray drying. A derived coating material was produced for the application as microwave absorbers using the as prepared powders by atmospheric plasma spray (APS) technology. The effects of $MoSi_2/Al_2O_3$ mass ratio on the dielectric and physical mechanical properties of the composite coatings were investigated. When the $MoSi_2$ content of the composites increases from 0 to 45%, the flexure strength and fracture toughness improve from 198 to 324 MPa and 3.05 to 4.82 $MPa{\cdot}m^{1/2}$ then decline to 310 MPa and 4.67 $MPa{\cdot}m^{1/2}$, respectively. The dielectric loss tangent increases with increasing $MoSi_2$ content, and the real part of permittivity decreases conversely over the frequency range of 8.2−12.4 GHz. These effects are due to the agglomeration of early molten $MoSi_2$ particles and the increase of the electrical conductivity with increasing $MoSi_2$ content.

Key words: $MoSi_2/Al_2O_3$ composite coating; atmospheric plasma spraying; mechanical properties; dielectric properties

1 Introduction

Radar absorbing materials (RAMs) are widely used in commercial and military applications. RAMs are made of compounds with high loss energy, which enables them to absorb the incident radiation in synchronized frequencies and dissipate it as heat [1]. At present, the most cost effective means of shielding radar radiation, controlling electromagnetic interference and dissipating electrostatic charge is to use magnetic or dielectric fillers [2] or intrinsically conducting polymers [3, 4]. Composite materials with different types of ferromagnetic or ferroelectric fillers have attracted much attention. $MoSi_2$ has potential applications varying from matrix material to reinforcing second phase for various high temperature structural applications due to its high modulus of elasticity, high melting point (2030 °C), superior oxidation resistance [5, 6], relatively low density (6.31 g/cm^3) , reasonably good electrical and thermal conductance (52 W/(mK)) [7, 8]. On the other hand, Al_2O_3 also has good oxidation and corrosion resistance because of its α-Al_2O_3 main crystalline phase, high melting point (2050 °C), and low density (3.7 g/cm^3). As the typical representative of low dielectric permittivity microwave dielectric ceramic, Al_2O_3 has perfect dielectric permittivity property, especially its low dielectric loss. ALFORD and PENN [9] and HUANG et al [10] reported the dielectric properties of the single phase Al_2O_3. When conductive inter-metallic compound $MoSi_2$ particles are introduced into Al_2O_3 matrix, not only the mechanical properties of Al_2O_3 composites can be enhanced, but also the dielectric loss and dielectric permittivity of the composites can be modified. Consequently, it is possible to provide the $MoSi_2/Al_2O_3$ composites with electromagnetic attenuation, but little attention is paid to its microwave absorbing properties. Because coating is the general form of RAM, efforts were focused on the preparation and dielectric properties of the $MoSi_2/Al_2O_3$ coatings by APS in this work. The complex permittivity, physical mechanical properties and possible mechanisms of the sprayed coatings were reported and discussed.

2 Experimental

Raw powders with different $MoSi_2$/ Al_2O_3 ratios (alumina produced by Hengjitianli Chemical Industry Co., Ltd. of Zibo，Shandong, China, Al_2O_3 ≥99.99%, average particle size of 40 μm; molybdenum disilicide

Foundation item: Project (50572090) supported by the National Natural Science Foundation of China; Project (KP200901) supported by the States Key Laboratory of Solidification Processing in NWPU, China
Corresponding author: WU Zhi-hong; Tel: +86-29-82202789, E-mail: wuzhihong@msn.com
DOI: 10.1016/S1003-6326(11)61148-5

produced by Dengfeng Electric Heating Industry Co., Ltd. of Henan, China, average particle size of 0.5 μm) were mixed in water with the addition of the organic binder system (poly vinyl alcohol, poly ethylene glycol, surfactant: Zschimmer & Schwartz Dolpapix CE64). The alumina mass fractions in these samples were 90%, 85%, 75%, 65% and 55%, marked as M1, M2, M3, M4 and M5, respectively.

After it was spray-dried, the composite powders of Al_2O_3 and $MoSi_2$ were obtained. Granularity analysis shows that the diameter of the composite powders is 45−75 μm. SEM photographs indicate that the dried powders have a $MoSi_2$-rich sheath and Al_2O_3-rich core. Figure 1 shows the typical microstructures of the composites with 15% (mass fraction) $MoSi_2$ after spray drying. Table 1 summarizes the compositions of slurries for spray drying.

Air plasma spray depositions of the processed powders were made on rough-surfaced graphite sheet substrates in order to easily get free-standing coatings. Plasma spraying was done with a non-transferred arc plasma torch operated at different power levels. The powders were fed at 16 g/min using argon as carrier gas. The plasma spraying parameters are listed in Table 2.

The density, microstructure, mechanical and dielectric properties were determined all on the free-

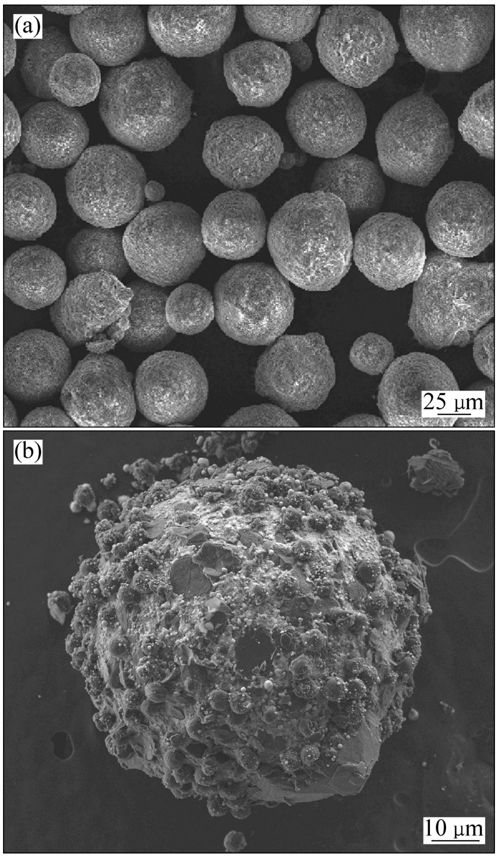

Fig. 1 SEM images of composite powders M2 after spray drying (a) and typical partied (b)

Table 1 Physical parameters of raw materials

Raw materials	Particle size/μm	Density/($g\cdot cm^{-3}$)	Elastic modulus/GPa
Al_2O_3	40	3.95	350
$MoSi_2$	0.5	6.24	440
Raw materials	**Electric conductivity/($\mu S\cdot cm^{-1}$)**	**Linear expansion coefficient/($10^{-6}K^{-1}$)**	**Melting point/°C**
Al_2O_3	6	5.6	2050
$MoSi_2$	−	7−8	2030

Table 2 Operating parameters of plasma spraying

Operating Power/kW	Plasma gas flow rate/($L\cdot min^{-1}$)	Powder
20	20	Molybdenum disilicide and aluminum
Powder size/μm	**Powder transporting gas flow rates/($L\cdot min^{-1}$)**	**Distance between torch and substrate/mm**
40−80	3	85−90

standing coatings. The densities were measured by Archimedes' method. The immersing liquid for density measurements was water, relative densities were calculated based on the rule of mixture, the bulk densities of Al_2O_3 and $MoSi_2$ were 4.0 and 6.2 g/cm^3, respectively. The flexure strength was measured with the three-point bending method. The fracture toughness was calculated with the indentation strength method.

Surface morphology was carried out by scanning electron microscopy (JSM−5610LV). The phase compositions were analyzed by full-automatic X-ray diffractometer (XRD). The dielectric parameters were carried out in the frequency range of 8.2−12.4 GHz by a network analyzer (Agilent Technology E8362B), which requires specimens are in dimensions of 10.16 mm×22.86 mm×2 mm.

3 Results and discussion

3.1 Physical mechanical properties

The density and flexure strength of the free-standing coatings with different $MoSi_2$ contents are shown in Fig 2. For comparison, samples with no $MoSi_2$ are also detected.

Figure 2 indicates that the relative densities of the $MoSi_2/Al_2O_3$ coatings decrease dramatically compared with the pure Al_2O_3 coating, which means that the addition of $MoSi_2$ into Al_2O_3 is detrimental to the sintering of the coatings. But with further increasing $MoSi_2$ content, the relative density of the $MoSi_2/Al_2O_3$ coatings increases gradually. It can be ascribed to the lower melting point and the higher thermal coefficient of

$MoSi_2$ than those of Al_2O_3, which improves the molten state of the dried grains during flight dwell and enhances the densities of the coatings.

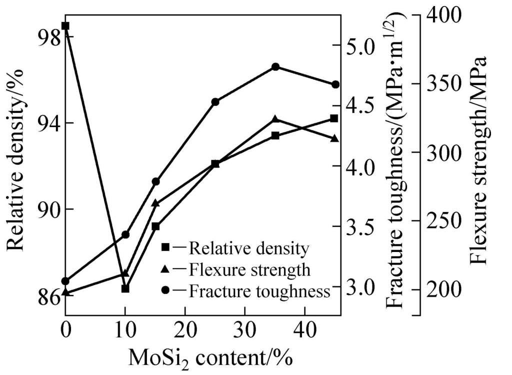

Fig. 2 Mechanical properties of $MoSi_2/Al_2O_3$ composition

The flexure strength and fracture toughness increase with the increase of $MoSi_2$ when the content is less than 35%. The reasons of the flexure strength variation with $MoSi_2$ content are summarized as follows. $MoSi_2$ particles can impede the growth of Al_2O_3 grains. High density of the coatings results from better melting state of sprayed particles; the grain-boundary energy and interfacial energy can be improved obviously by adding $MoSi_2$, and as the content increases, the effect becomes more significant [11]. The fracture toughness increase with $MoSi_2$ content is resulted from finer Al_2O_3 grains and microcracks between Al_2O_3 and $MoSi_2$ grains due to their different thermal expansion coefficients [12]. When the $MoSi_2$ content reaches 45%, the flexure strength and fracture toughness all decline, because the effect of Al_2O_3 matrix is weakened.

3.2 Phase of composite coatings

The XRD patterns of the free-standing coatings are shown in Fig. 3.

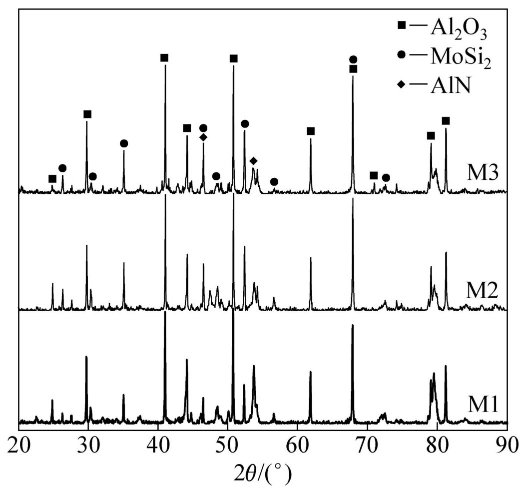

Fig. 3 XRD patterns of $MoSi_2/Al_2O_3$ composite with different $MoSi_2$ contents

It is seen that the dominating phases are $MoSi_2$ and Al_2O_3. In addition, new AlN phase is found. This is because nitrogen (N_2) is used as shielding gas and reaction gas during plasma spraying process. It reacts with Al_2O_3 on the surface of graphite substrate to form AlN. The possible reaction to produce AlN is [13, 14]

$$Al_2O_3 + N_2 + 3C = 2AlN + 3CO\uparrow$$

In this case, it can be found that AlN is produced by Al_2O_3, C (from the graphite substrate) and N_2 (spraying atmosphere). Considering the small amount of AlN, the effect of this third phase on the dielectric performance of the composite studied in this work should be negligible.

3.3 Microstructure of composite coating

Figure 4 shows the typical microstructures of the composites with 10%, 15% and 25% (mass fraction) $MoSi_2$ after polishing the surface of the samples.

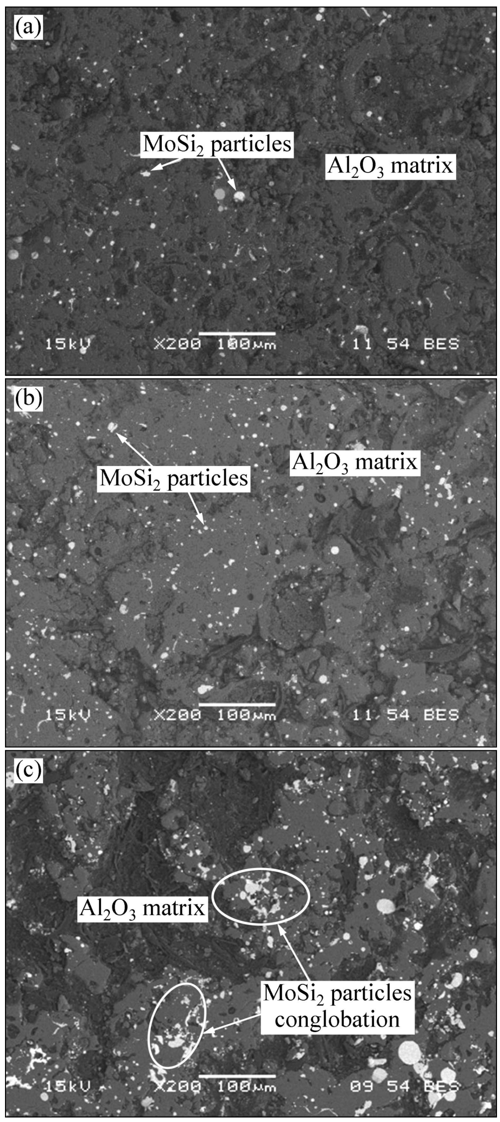

Fig. 4 SEM images of coatings after APS with different $MoSi_2$ contents: (a) M1; (b) M2; (c) M3

From Fig. 4, it is apparent that the composites contain some black matrix materials and some speckled black phases. The XPS X-ray photoelectron spectroscopy result indicates that the black phase contains 65.3% Si (molar fraction) and 32.5% Mo. Hence, it is molybdenum disilicide. It can be found from Fig. 4 that $MoSi_2$ particles are homogeneously distributed in the Al_2O_3 matrix and along with the increase of the $MoSi_2$ content, this distribution is more apparent. But at the same time, there are some conglobation and adhesion of $MoSi_2$ particles, which is mainly due to two aspects. On one hand, some of the $MoSi_2$ particles on the surface of Al_2O_3 particles can congregate during spray drying granulation. On the other hand, in the plasma spray process, the $MoSi_2$ particles melt more completely than Al_2O_3 particles. The molten $MoSi_2$ is inclined to form partial clustering by capillary forces.

3.4 Dielectric properties

The real parts of permittivity (ε') and dielectric loss tangent properties ($\tan\delta$) of the $MoSi_2/Al_2O_3$ coatings sprayed using different amounts of $MoSi_2$ powders are shown in Figs. 5(a) and (b), respectively. From Fig. 5(a), it can be seen that the ε' of the $MoSi_2/Al_2O_3$ composites decreases with the increase of $MoSi_2$ content across the whole frequency range. The ε' presents an obvious decrease from 8−11.3 to 5−8.4 in the tested frequency range when $MoSi_2$ content increases from 10% to 45%. With the same $MoSi_2$ content, ε' also slightly decreases with increasing frequency which indicates that the composite material has some frequency dispersion. It is generally known that ε' reflects the capability of store charge of materials. According to the principle of equivalent circuit, the real parts of $MoSi_2/Al_2O_3$ permittivity vary directly with the surface area of $MoSi_2$ particles. As mentioned before, increased $MoSi_2$ content might promote the clustering of $MoSi_2$ particles in the $MoSi_2/Al_2O_3$ composites (as shown in Fig. 4), expanding the $MoSi_2$ particles surface. When the content of $MoSi_2$ increases from 10% to 45%, the specific surface area decreases, the real parts of permittivity descend. From Fig. 5(b), it can be seen that the value of loss factor in $MoSi_2/Al_2O_3$ composites increases with increasing $MoSi_2$. This is because the dielectric loss of $MoSi_2/Al_2O_3$ composite relates to its electrical conductivity. As known, $MoSi_2$ has high electrical conductivity. When $MoSi_2$ particles are dispersed in Al_2O_3 matrix, a $MoSi_2$ conductive network can be formed [15]. When the interparticle distance is shorter than the gap width that quantum tunneling effect permits, conductive networks form. For composites blending with dispersed spherical particles, MARGOLINA and WU [16] assumed a simple cubic lattice to calculate the surface-to-surface interparticle distance as:

$$\delta = D\left[\left(\frac{\pi}{6\varphi}\right)^{1/3} - 1\right] \tag{1}$$

where δ is the average surface-to-surface interparticle distance; D is the particle diameter and φ is the volume fraction of particles. Equation (1) shows that the δ of the $MoSi_2$ particles is dependent on the volume fraction as the particle diameter is constant. This can be observed in the SEM images (Fig. 4) of the composites with different $MoSi_2$ contents. The distances between the $MoSi_2$ particles are shortened by increasing $MoSi_2$ content. At the same time, the $MoSi_2$ agglomerations also increase due to the increasing possibility of the contact between $MoSi_2$ particles as the proportion of $MoSi_2$ increases. The schematic of $MoSi_2/Al_2O_3$ composites with different $MoSi_2$ contents is shown in Fig. 6. The average surface-to-surface interparticle distance of filled particles in high $MoSi_2$ content composites is relatively short. This means that the high $MoSi_2$ content is more likely to reach the critical surface-to-surface interparticle distance (i.e. the electron hopping gap width) based on Eq. (1). The $MoSi_2$ particles in high $MoSi_2$ content composites are more prone to form conductive networks. Therefore, with increasing $MoSi_2$ content, the electrical conductivity and $\tan\delta$ both increase.

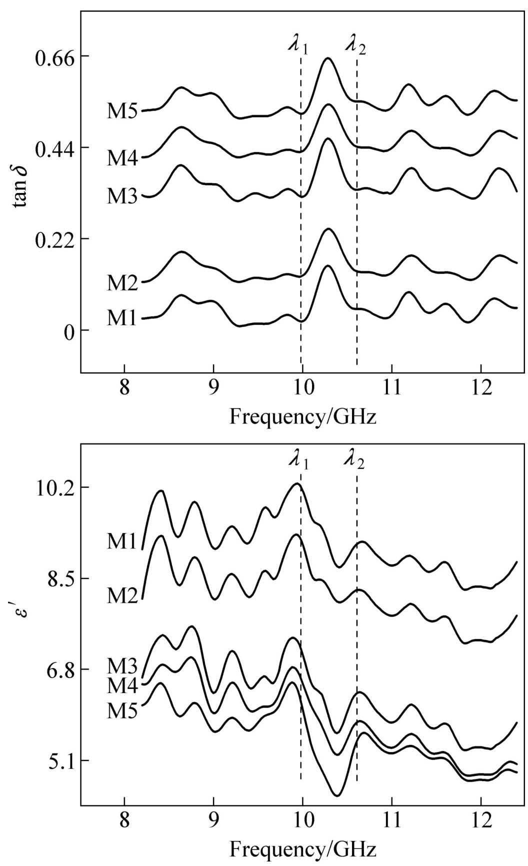

Fig. 5 Complex permittivity (a) and dielectric loss tangent (b) vs frequency of different $MoSi_2$ composite coatings

The real permittivity and dielectric loss tangent value show an obvious fluctuation between 10 and 10.5 GHz among the lines λ_1 and λ_2, as shown in Fig. 5. This phenomenon can be interpreted as the correlated relationship between the real permittivity (polarization) and imaginary permittivity (electric loss), i.e., energy storage (capacitor) $\longleftrightarrow$ energy dissipation (resistor). Similar results were reported in the other filled composites [17, 18].

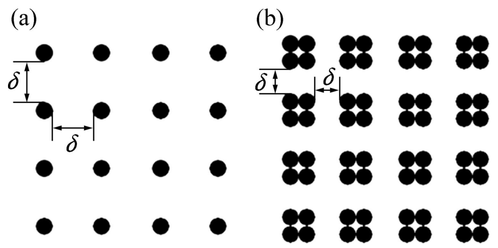

Fig. 6 Schematic diagrams of different $MoSi_2/Al_2O_3$ composites: (a) Low content of $MoSi_2$; (b) High content of $MOSi_2$

4 Conclusions

1) The spray drying method can effectively let $MoSi_2$ cover the surface of the Al_2O_3 core particles and isolate its contact with each other.

2) The $MoSi_2$ particles are homogeneously distributed in the Al_2O_3 matrix, but the appearance of some conglobation occurs with increasing $MoSi_2$ contents. These are due to the congregate of $MoSi_2$ particles on the surface of Al_2O_3 core particles during spray drying granulation and partial clustering by capillary forces during APS.

3) The decrease of the real parts (ε') of permittivity is mainly caused by the agglomeration of early molten $MoSi_2$ particles, and the increase of the dielectric loss tangent properties (tan δ) of the $MoSi_2/Al_2O_3$ coatings is due to the increase of the electrical conductivity with increasing $MoSi_2$ content.

4) The mechanical properties can be tailored by choosing a suitable $MoSi_2$ content. $MoSi_2/Al_2O_3$ composite is a promising material in both the electro-magnetic absorption characteristics and the load-bearing capacity aspects.

References

[1] FAN Z J, LUO G H, ZHANG Z F, ZHOU L, WEI F. Electromagnetic and microwave absorbing properties of multi-walled carbon nanotubes/polymer composites [J]. Mater Sci Eng B, 2006, 132(1−2): 85−89.

[2] MAEDA T, SUGIMOTO S, KAGOTANI T, TEZUKA N, INOMATA K. Effect of the soft/hard exchange interaction on natural resonance frequency and electromagnetic wave absorption of the rare earth-iron-boron compounds [J]. J Magn Magn Mater, 2004, 281(2−3): 195−205.

[3] SOTO-OVIEDO M A, ARAÚJO O A, FAEZ R, REZENDE M C, de PAOLI M A. Antistatic coating and electro-magnetic shielding properties of a hybrid material based on polyaniline/organoclay nanocomposite and EPDM rubber [J]. Synthetic Met, 2006, 156(18−20): 1249−1255.

[4] WOJKIEWICZ J L, FAUVEAUX S, MIANE J L. Electromagnetic shielding properties of polyaniline composites [J]. Synthetic Met, 2003, 135−136: 127−128.

[5] JENG Y L, LAVERNIA E J. Processing of molybdenum disilicide [J]. J Mater Sci, 1994, 29(10): 2557−2571.

[6] YAN Jian-hui, ZHANG Hou-an, XU Hong-mei, WU Hai-jiang, TANG Si-wen. Preparation of $MoSi_2$ powder used for plasma-spraying and its melting characteristics in plasma arc [J]. The Chinese Journal of Nonferrous Metals, 2011, 21(4): 836−842. (in Chinese)

[7] LIN W Y, HSU J Y, SPEYER R F. Stability of molybdenum disilicide in combustion gak environments [J]. J Am Ceram Soc, 1994, 77(5): 1162−1168.

[8] PETROVIC J J. Mechanical behavior of $MoSi_2$ and $MoSi_2$ composites [J]. Mater Sci Eng A, 1995, 192−193(Part 1): 31−37.

[9] ALFORD N M, PENN S J. Sintered alumina with low dielectric loss [J]. J Appl Phys, 1996, 80(10): 5895−5898.

[10] HUANG C L, WANG J J, HUANG C Y. Sintering behavior and microwave dielectric properties of nano alpha-alumina [J]. Mater Lett, 2005, 59(28): 3746−3749.

[11] NEWMAN A, SAMPATH S, HERMAN H. Processing and properties of $MoSi_2$−SiC and $MoSi_2$−Al_2O_3 [J]. Mater Sci Eng A, 1999, 261(1−2): 252−260.

[12] Aikin R M. Structure and properties of in situ reinforced $MoSi_2$ [C]//Wachtman J B. Proceedings of the 15th Annual Conference on Composites and Advanced Ceramic Materials: Ceramic Engineering and Science Proceedings. Hoboken, NJ, USA: John Wiley & Sons, Inc., 2008: 1643-1655.

[13] LI Z J, PAN X L, SUN W M, QU J H, WANG F. Production and character of Al_3O_3N nanowires [J]. Acta Phys Sin-ch Ed, 2005(1): 450−453.

[14] CAO Zhong-liang, WANG Zhen-yun. The manual of inorganic chemistry reaction equations [M]. Changsha: Proceedings of the Fourth Inte Science Press, 1985: 150−151. (in Chinese)

[15] HUANG Z B, ZHOU W C, TANG X F, ZHU J K. Effects of milling methods on the dielectric and the mechanical properties of hot-pressed sintered $MoSi_2/Al_2O_3$ composites [J]. J Alloy Compd 2011, 509(5): 1920−1923.

[16] MARGOLINA A, WU S H. Percolation model for brittle-tough transition in nylon/rubber blends [J]. Polymer, 1988, 29(12): 2170−2173.

[17] WATTS P C P, PONNAMPALAM D R, HSU W K, BARNES A, CHAMBERS B. The complex permittivity of multi-walled carbon nanotube- polystyrene composite films in X-band [J]. Chem Phys Lett, 2003, 378(5−6): 609−614.

[18] RAMIREZ A P, HADDON R C, ZHOU O, FLEMING R M, ZHANG J, McCLURE S M, SMALLEY R E. Magnetic susceptibility of molecular carbon: nanotubes and fullerite [J]. Science, 1994, 265(5168): 84−86.

$MoSi_2$ 含量对 $MoSi_2/Al_2O_3$ 复合涂层介电与力学性能的影响

武志红，周万城，罗 发，朱冬梅

西北工业大学 凝固技术国家重点实验室，西安 710072

摘 要：通过喷雾干燥法制备 $MoSi_2$ 包覆 Al_2O_3 的壳核结构混合粉，利用该混合粉以等离子喷涂技术制备 $MoSi_2/Al_2O_3$ 复合涂层材料。研究 $MoSi_2/Al_2O_3$ 质量比涂层材料的力学和介电性能的影响。结果表明：随着 $MoSi_2$ 含量从 0 增加到 45%，复合材料的抗弯强度和断裂韧性分别从 198 MPa 和 3.05 $MPa\cdot m^{1/2}$ 增加到 324 MPa 和 4.82 $MPa\cdot m^{1/2}$，随后又降到 310 MPa 和 4.67 $MPa\cdot m^{1/2}$。在 8.2−12.4 GHz 微波频率波段内，随着 $MoSi_2$ 含量的增加，复合材料的介电损耗增加，而介电常数的实部却呈减小趋势。这主要是由于 $MoSi_2$ 颗粒熔化后的凝聚及导电网络结构的形成导致电导率的增加引起的。

关键词：$MoSi_2/Al_2O_3$ 复合涂层；大气等离子喷涂；物理力学性能；介电性能

(Edited by FANG Jing-hua)